

# Numerical Modeling of a Wing Skin Peen Forming Process

R.D. VanLuchene and E.J. Cramer

For many years shot peening has been used to provide fatigue resistance and form to airplane wing skins at the Boeing Commercial Airplane Company. In this process, the peening intensities used to form a new wing skin have been obtained through the use of approximate geometric relationships, along with a considerable amount of trial and error testing. This paper describes a numerical model that has been applied to replicate the shot peening process used at Boeing. The model is used to predict peening intensities and the initial size of the skin (flat pattern) given an arbitrary aerodynamic contour requirement. Discussion focuses on the finite element method and special optimization techniques used in the approach.

## Keywords

optimization, shot peening, wing skins

## 1. Introduction

WHEN THE SURFACE of a metal part is repeatedly hit at a high velocity by small steel shot, a thin plastically deformed layer is formed beneath the impacted area. For many years, it has been known that the residual surface stresses after this peening process are compressive. Figure 1 qualitatively shows the resulting residual stress distribution when a relatively thin metal part is impacted. In this figure,  $h_p$  represents the thickness of the plastic layer. The residual stresses shown are of considerable benefit in improving the resistance of the metal to fatigue and stress corrosion cracking resulting from exposure to cyclical loads. Metal parts which have often been shot peened for this effect are axles, springs, aircraft landing gear, and structural parts (Ref 1-5).

More recently, shot peening has been used to provide curvature to metal parts of small stiffness, such as airplane wing skins. This process is called peen forming and results in benefits of both fatigue resistance and form. In the peen forming process, one or both sides of the thin part is impacted with varying shot kinetic energy so that the part obtains a desired contoured shape. The following discussion provides insight into the basic physics of the shot peening process and the details of the numerical model that approximates the physics.

### 1.1 Shot Impact Physics

As noted above, uniform shot impact produces a thin, plastically deformed layer with thickness  $h_p$  beneath the peened surface. The plastically deformed layer causes the metal to undergo two basic geometric changes in order to reach equilibrium. The top layer elongates in order to alleviate the compressive stress, and the growth creates a stress differential through the thickness of the metal part. This differential causes the metal part to curve in the direction of the peened surface to maintain equilibrium, as shown in Fig. 2. Any numerical

method used to approximate the shot peening process must therefore be capable of producing both the bending and stretching effects shown in Fig. 2.

Up to this point, the discussion has assumed that the plastic layer  $h_p$  is relatively small compared to the part thickness. The plastic layer, however, may be increased by increased shot size or impact velocity. It has been experimentally verified that  $h_p$  reaches a critical value where the "deflection" shown in Fig. 2 is maximized. Further increases in  $h_p$  result in decreases in the arc height. It has also been found that large values of  $h_p$  actually cause the part to deflect in the direction of shot flow, i.e., in the direction opposite that shown in Fig. 2. While this phenomenon is interesting, it need not be considered in the model presented here. In order to develop these larger values of  $h_p$ , the resulting impacted surface becomes unacceptably rough from an aerodynamic point of view, and therefore the process is not acceptable.

### 1.2 Previous Developments and Limitations

There have been attempts to quantify the stress distribution shown in Fig. 1 (Ref 7, 8). The models developed require test data to "tune" their prototype parameters. The method developed here takes a different approach, using a finite element model with a linear elastic material so that determination of the residual stress pattern of Fig. 1 is not necessary. What is necessary, however, is quantification of the induced stresses resulting from shot peening a totally constrained or fixed "element." A simple model for doing this is presented in another paper under development.

At the Boeing Company, previous methods for determining the peening pattern for a new aircraft wing skin had limitations involving: (a) finding the initial flat shape (flat pattern) of the wing skin before peening, so that it ends up the correct size after it has undergone the growth and curvature associated with peening, and (b) obtaining the correct peening intensities across the skin without trial and error. The methods used to predict the initial flat shape involved no knowledge of the intensity patterns that were used and clearly affect the material growth. In addition, the methods used to predict the peening intensity were purely geometric in nature and did not enforce basic mechanics relationships that were developed from equilibrium and compatibility, and that satisfy material constitutive relationships.

R.D. VanLuchene, Department of Civil Engineering, Montana State University, Bozeman, Montana, USA; and E.J. Cramer, Boeing Commercial Airplane Company, Seattle, Washington, USA.

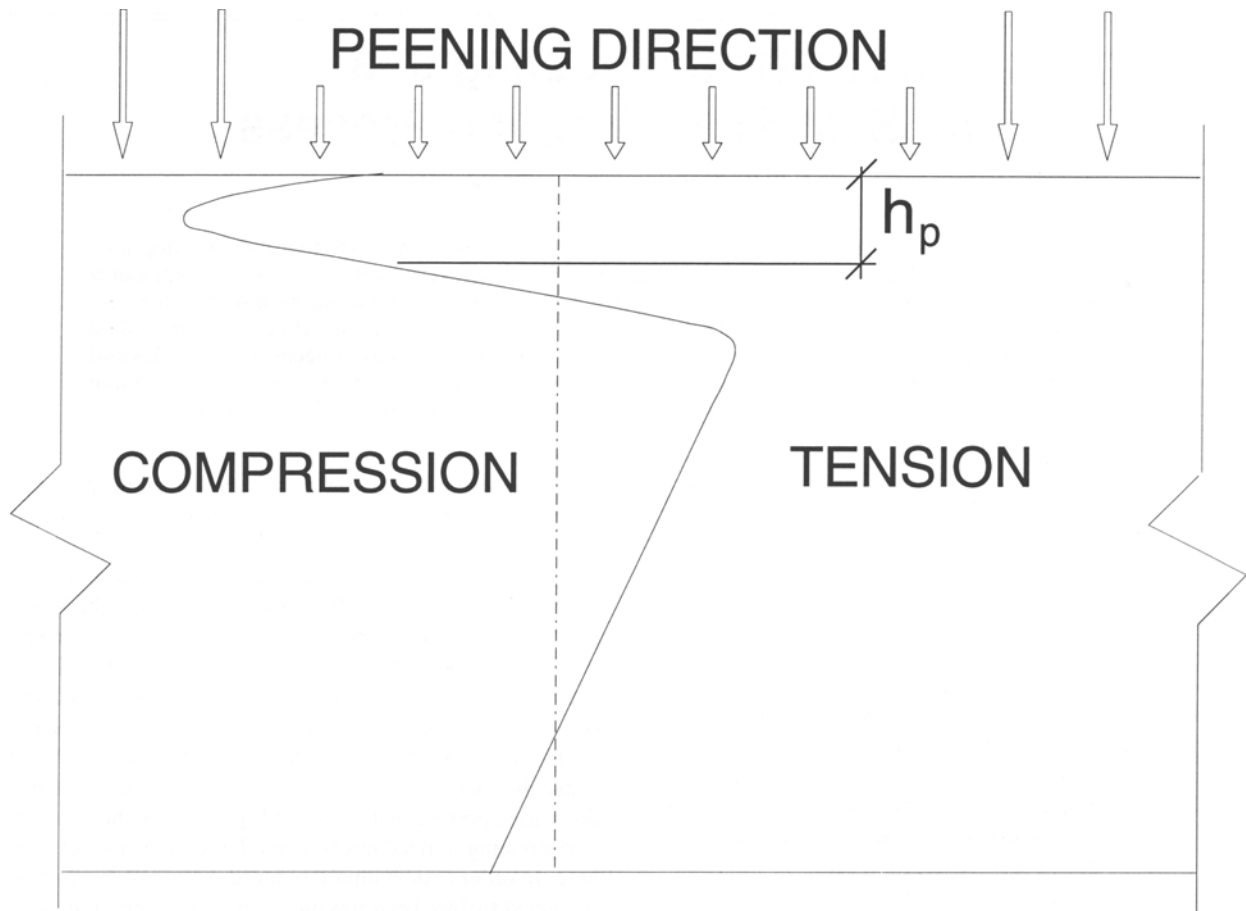


**Fig. 1** Residual stress distribution after shot peening one side of a thin part

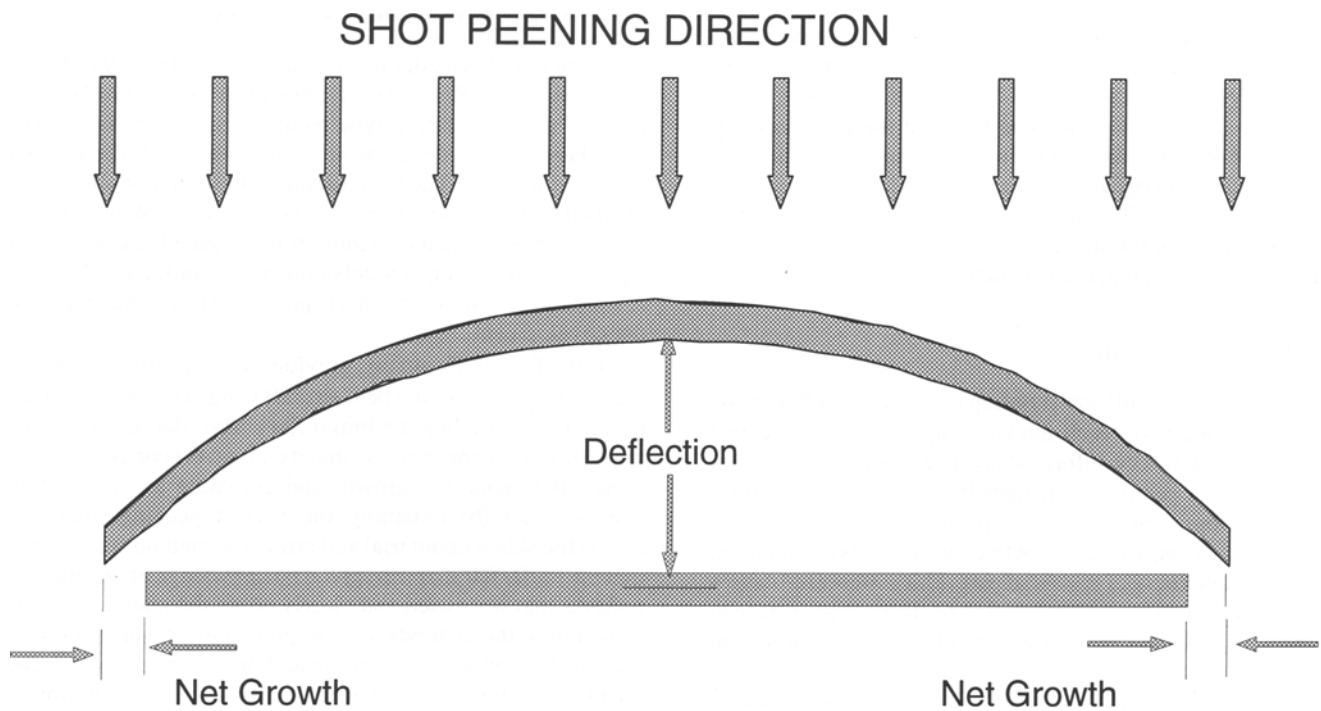


**Fig. 2** Growth and curvature from shot peening on one side of a part. Source: Ref 6

The work presented in an earlier paper (Ref 6) is based on a prototype model of the shot peening process utilizing the finite element method. The model presented here follows the basic approach detailed in Ref 6, but there were several shortcomings in that earlier work. First, no provision was made for developing the initial flat pattern based on the peening intensities. The work also neglected the effects of gravity on the shape, a phenomenon called "drape" in this paper. Several other finite element considerations were enhanced in the work described here. Finally, this paper emphasizes the optimization considerations that are an integral part of the numerical model.

## 2. Numerical Process Model

The successful application of the finite element method to solid mechanics problems has been well documented. The numerical model proposed here also relies heavily on finite element techniques and employs thin shell theory finite elements. Figure 3 is a flow chart of the computational modules used. As can be seen, there are four processing modules in the proposed system: a model setup module, a drape processor, a finite element module, and an optimization module. These are described in separate sections below. (Discussion of the skin geometry definition is beyond the scope of this paper. At Boeing, these data are generated by computer-aided design software such as CATIA (The Boeing Company, Seattle, WA). Also, the format of the resulting output, which includes both peening intensity data and flat pattern data, is not presented.)

### 2.1 Finite Element Setup Module

The first computational module used in this system is responsible for setting up the finite element model used in the remainder of the analysis. Meshing is assumed to have been done previously, and results are included in the skin geometry definition provided to the setup module. Two basic tasks are performed by the setup module: establish a least squares fit plane, and establish a supporting system for the finite element model. These tasks are critical to the overall performance of the system.

When the setup module receives geometry information, it is assumed to be in an arbitrary coordinate system, say  $X'Y'Z'$  as shown in Fig. 4. This system usually corresponds to a physical aircraft coordinate system. For the analysis described here, a coordinate system is established such that the XY plane corresponds to the plane that the flat or unpeened part lies in. Z coordinate motions therefore are assumed to move the flat part into the final required aerodynamic contour. The mapping between the physical coordinate system and the XY flat plane is assumed to be done such that the XY plane is a least squares best fit plane through the contoured shape. This is depicted in Fig. 4. The rationale for choosing the least squares plane is that it represents the position where a flat part would have to be displaced least to achieve the contour. It follows that peening effort would be nearly minimized if the required forming displacements were chosen in the same manner.

With XYZ coordinates determined for the contoured wing skin, the second task of the setup module is to establish a supporting scheme for the skin during a finite element analysis

simulating shot peening. The supporting scheme should not affect analysis results and simply needs to provide the necessary kinematic stability to the model, i.e., eliminate rigid body translations and rotations about the X, Y, and Z axes. Two schemes were studied: a three-point system similar to a three-legged table, and a single-point support. There are advantages and disadvantages to both schemes. For the three-point support, all six rigid body motions are easily handled by having all three points with translational Z, one point with translational X, and one point with translational Y (provided all points are not collinear). For this scheme, the most stability (both physical and numerical) is found by maximizing the distance between the points. This tends to be difficult for long, narrow wing skins whose length-to-width ratios approach 20:1.

The single-support scheme requires constraining all translations and rotations of a single point in the finite element model. For stability, a point near the center of the part is chosen. Unlike the three-point scheme, the single-point scheme requires that the thin shell finite elements used possess in-plane or "drilling" stiffness for the model to have Z rotational stability. This stiffness is not common in typical thin shell elements. For this reason, two nontypical shell finite element formulations were considered with the single-point scheme. The first was proposed by Zienkiewicz (Ref 9) as a simple "add on" to a standard thin shell finite element to provide drilling stiffness. Our results using this approach were not accurate and were very sensitive to the required input stiffness parameter. Recently, more advanced methods have been proposed for inclusion of drilling stiffness in shell elements (e.g., Ref 10). Based on our experience, these element formulations provide acceptable results for the single-point support scheme.

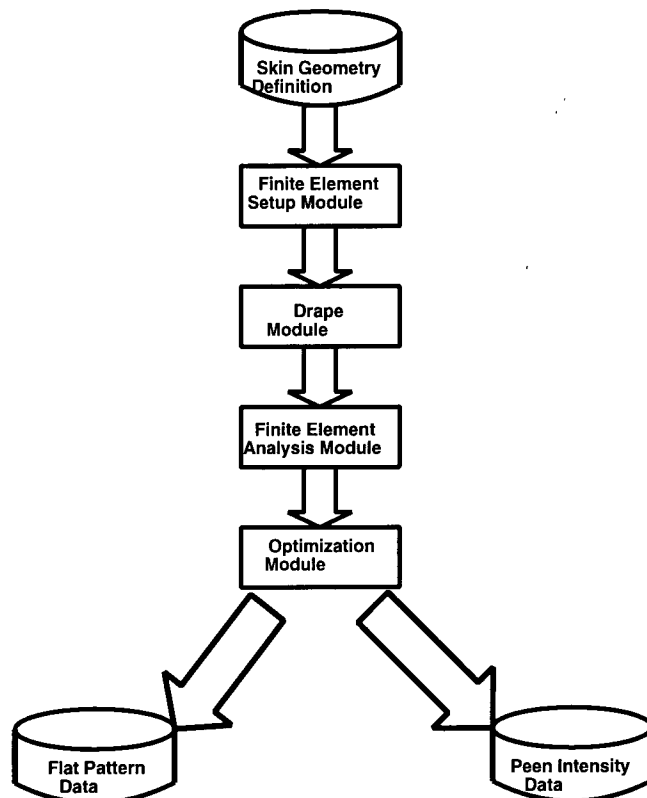


Fig. 3 Software module flow chart

When comparing both support schemes, it was found that the solution sensitivity to support point location was much less in the single-point scheme than in the three-point scheme. Also, for the sake of simplicity, it was easier to establish a single point near the center of the mesh than to establish three whose distance apart was maximized. Presently, therefore, the system utilizes the single-point support scheme for providing kinematic stability. The thin shell element formulations are based on the work cited in (Ref 10) above.

## 2.2 *Drape Module*

Gravitational effects have a positive impact on how well a wing skin fits a required aerodynamic contour. Wing skins have relatively low stiffness and are placed upon a formed surface where the form is usually provided by other structural members, such as spars and stringers. Gravity causes the part to naturally come to form, and this effect is termed *drape*. The amount of contour that can be achieved is a function of the thickness (stiffness) of the wing skin and the degree of curvature required by the contour. For thin parts placed on low-curvature wing contours, all or nearly all contour is achieved by drape, and shot peen forming is not needed. For thicker wing skins, drape still affects the fit positively by allowing parts to be slightly under- or overcontoured. The purpose of the drape module is to quantify the positive impact of drape on the overall shot peening process. The premise here is that if drape effects are considered, overall shot peening effort should be reduced somewhat over that of a numerical model which neglects drape.

The approach involves simulating the laying of a partially peened part down upon a solid contact surface. This is most easily visualized by imagining a flat wing skin part being lowered onto the spar-stringer arrangement for the wing. It is assumed that the part is lowered in a level position (keeping Z constant) until the location with largest Z contour value contacts the flat part. The part is then assumed to pivot about this point until a second contact point is established. Finally, as the part pivots about the line established by these two points, a third contact point is located. With three contact points established, a kinematically stable structure exists and a gravity analysis can be performed. Computationally, these three contact points are established by first locating the point with largest Z contour. An exhaustive search is then begun, using all the remaining possible nodal point pairs to establish a plane. If this plane passes through the contour, it is rejected. This search method is not computationally optimized, but it represents only a small fraction of the overall computational requirement. Furthermore, a unique solution (plane) cannot be guaranteed, but this is not critical due to the approximate nature of the drape handling as a whole.

With the initial three contact points established, an incremental finite element analysis is initiated. The gravitational load is applied in small steps, and as this is done, points of the skin come into contact with the established contoured surface. As the contact is made, spring contact elements are added to the finite element model, and solution proceeds. As with any general contact problem, it is necessary to check at each iteration for tensile spring forces indicating that the skin is raising off the test surface. When these are detected, the springs are removed

from the model. When all the load steps required to provide full gravity loading are applied, the originally flat part has come in partial contact with the contoured surface. As mentioned above, if the part is sufficiently thin and the contour nearly flat, full contact will be possible after the incremental loading. Loading steps are held small, and equilibrium iteration within each load increment is not performed as is commonly done in a general nonlinear finite element analysis.

The results of the analysis performed above leads to a set of nodal Z coordinate deviations between contour and final part resting place after gravity load application. Initially these deviations were used as the required Z coordinate displacements to be provided by shot peening. This approach, however, led to peening patterns which were not smooth and also were largely unlike any patterns developed in the past. Also, the method above errs in assuming that the part is flat as it is being lowered into its final resting place on spars and stringers. In reality, the skin has been peened and has some initial contour which directly affects drape deflections, making them different from that of an initially flat part. A change in the approach was therefore needed.

The actual drape calculation method used is as follows. It is assumed that the required Z coordinate displacements to be provided by shot peening will be in direct proportion to the contour shape. In other words, the drape module determines a single drape factor which uniformly scales the full contour Z coordinates back to smaller values. This recognizes the beneficial effects of drape, but in a conservative manner. This method has the added advantage of preserving smooth peening pattern solutions (assuming smooth contour shapes). The single drape factor is calculated iteratively as follows. A drape factor is assumed, say 5% (in other words, peening must provide 95% of the Z contour coordinate). A part with a shape of 95% of the contour is then assumed to be lowered onto the full contour surface. Contact points are calculated and an incremental analysis is performed as described above. If all points end up in contact with the full contour surface at full gravity loading, the drape factor is increased. The analysis is repeated until a drape factor is chosen where the part "just" contacts the full contour surface at full gravity loading. The actual method for determining the final drape factor employs a simple bisection algorithm which leads to reasonable convergence. A better convergence method could have been chosen, but, these calculations represent a small fraction of the overall effort.

Experience with typical wing skins at Boeing indicates that the drape factor is usually around 5%. This factor indirectly reduces the required peening intensity by a similar amount. It should be emphasized that this is a conservative approach to considering the drape effect. In reality, drape can provide even more contour development, but this will be at the expense of less smooth and less intuitive peening patterns.

## 2.3 *Finite Element Analysis Module*

The finite element analysis module is responsible for generating the input data to the optimization software described below. The input data consists of a set of influence factors that indicate how peening affects the contour development of the wing skin. In order to properly develop the behavior shown in Fig. 2, individual finite elements are assumed to undergo both

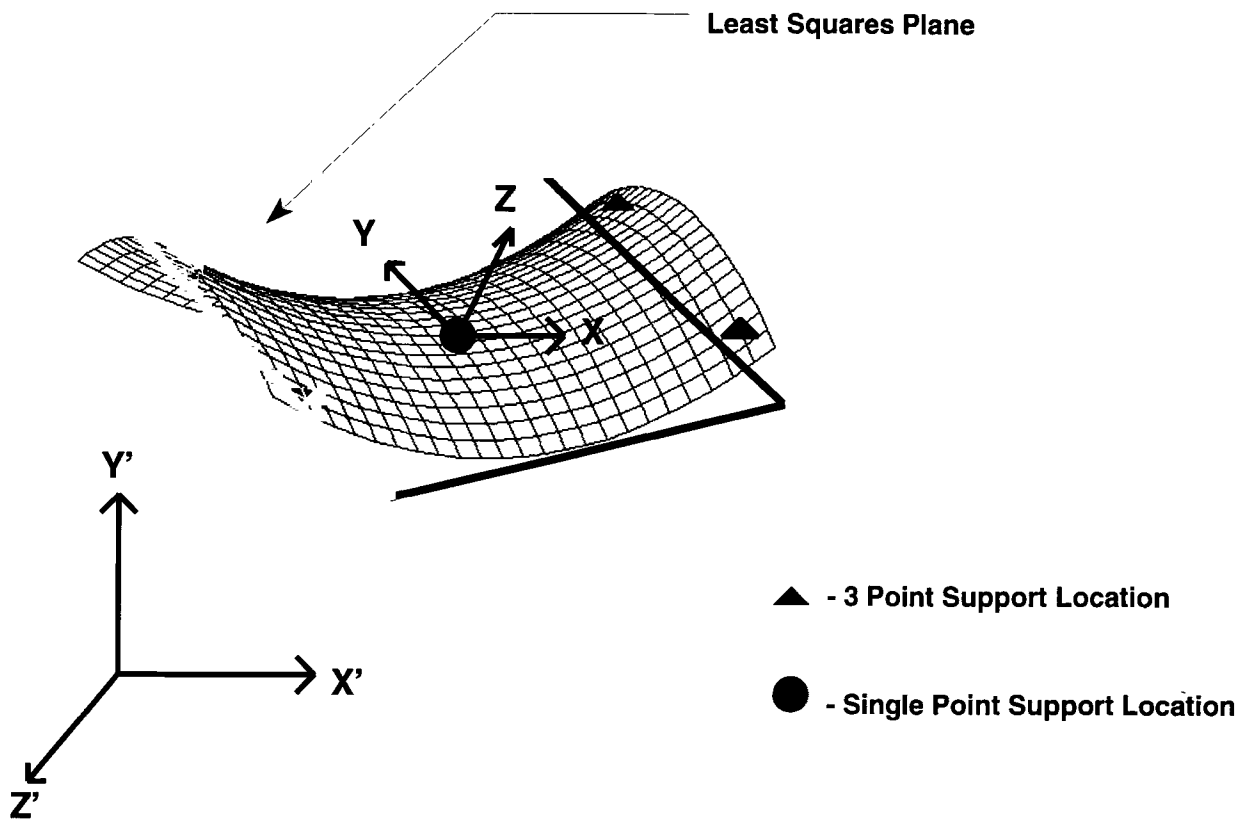


**Fig. 4** Flat part coordinate system

unit membrane stress and unit bending stress loadings. Graphically, these stresses may be represented as shown in Fig. 5. In the formulation presented here, the basic problem to be solved is the determination of the linear combination of these stress influences for all finite elements in the model. The scale factors for each influence directly relate to shot peening intensity over that element. Several objectives must be satisfied by this combination, and these are discussed in more detail in the optimization section below. This section summarizes the details involved with the creation of these unit stress influences.

Many aspects are considered part of an accurate finite element solution. Wing skins can be assumed to behave as thin shells with negligible shear deformation. Section 2.1 above summarizes the finite element model as a discretization of the wing skin into a grid of quadrilateral plate/shell elements. A typical grid is shown in Fig. 4. Stability of the model is provided by a single-point constraint where all degrees of freedom are specified to be zero. This type of support therefore necessitates the use of an element formulation with drilling degrees of freedom.

In deforming from an original flat geometry to the final contoured shape, elements in the finite element model may undergo rotations which can be classified as large in a finite element context. Special handling is necessary so that correct strains can be calculated based on these rotations. In further classifying the problem of wing skin deformation during shot peening, it has been observed that the required deformations can be achieved by small elastic strains. The use of large strain measures is therefore unnecessary as long as the large rotations are properly handled. In order to satisfy these requirements, the

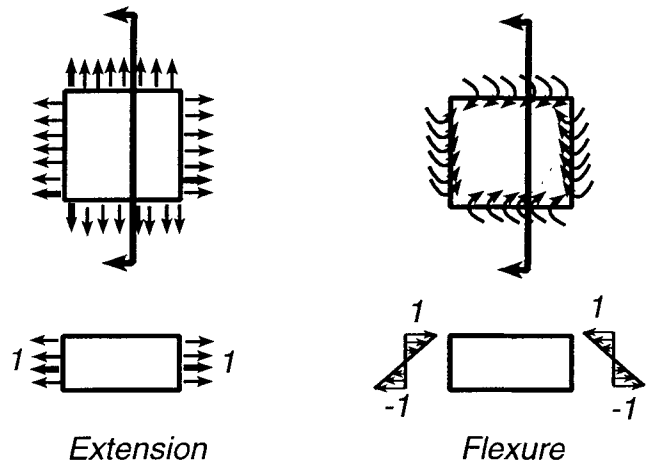


**Fig. 5** Unit stress influences

finite element module used in this development employs a convected coordinate approach to solving the large rotation/small strain problem. This approach is summarized in Ref 11 and 12.

Another question which has been addressed in this work involves the proper configuration to use for estimating the stiffness and response to the effective stresses of Fig. 5 during the peening simulation. This issue arises due to the change in configuration during the peening process, i.e., as the wing skin is peened, its shape changes from flat to contoured, and therefore its response to the effects of peening also changes. Because of the complex and often uncontrollable order in which various sections of the skin are actually peened, modeling the process

in the time domain allowing a changing configuration is not computationally feasible.

The peening patterns produced based on the two extremes of skin configuration (flat and fully contoured) were compared for several production wings at Boeing. Considerably different patterns were predicted in each case, which is not surprising. For the flat configuration, a stretching produces no motion perpendicular to the skin. However, if the configuration follows the contour, an extension produces a component of deflection which aids directly in contour development. When the patterns developed were studied closely, it was concluded that the final configuration model produced patterns closest to those presently in use. For further verification, a cylindrical wing skin was peened using the patterns produced from each configuration. Results of this test revealed that the fully contoured configuration provided a significantly better peening pattern. The finite element module of this development therefore uses the fully contoured configuration for estimating the stiffness and response to the effective stresses of Fig. 5.

Based on the assumptions stated above, the finite element module performs a static analysis of the wing skin. A set of nodal deflections are calculated for a unit stretching and a unit bending stress assumed to be applied to each element in the model. If there are  $N$  finite elements in the model, then  $2N$  sets of nodal deflections are obtained. From an efficiency point of view, stiffness is formed and decomposed only once during the process, allowing a forward elimination and back substitution for each loading situation. It is also noted that the large rotation corrections can be performed without iteration, because the final configuration (wing contour) is known. This precludes the use of an iterative procedure as normally used in nonlinear finite element problems. The next section discusses the optimization problem which directly operates on the deflection sets calculated by the analysis module.

### 3. Optimization Module

This section describes how finding the intensity pattern for the shot peening problem can be formulated as a linearly constrained least squares (LCLS) problem in a form compatible with LSSOL (Least Squares Solution Optimization Library; Ref 13). The template for the LCLS problem is the following:

LCLS:

Find  $x$  (variables) to minimize

$$c^T x + \frac{1}{2} \|Ax - b\|^2 \text{ (objective function)}$$

$$\text{subject to } \begin{cases} l \leq x \leq u & \text{(bounds)} \\ p \leq Cx \leq q & \text{(constraints)} \end{cases} \quad (\text{Eq 1})$$

In section 3.2 we discuss what peening parameters to substitute in Eq 1 for  $c, A, b, l, u, p, C$ , and  $q$ .

Although we are currently solving the problem as an LCLS, much of the following discussion could be generalized to a nonlinear constrained problem. Other optimization packages can also be used to solve the LCLS problem (Ref 14). A more

detailed discussion of optimization for shot peening can be found in Ref 15.

Sometimes it may be advantageous to find a set of variables that satisfy the constraints without considering an objective function. Such a point is called a feasible point (FP) and is found by solving:

FP:

$$\text{Find } x \text{ to satisfy } \begin{cases} l \leq x \leq u \\ p \leq Cx \leq q \end{cases} \quad (\text{Eq 2})$$

#### 3.1 Characteristics of a Good Pattern

The following is a list of possible characteristics of a good pattern and how they can be written with mathematical notation. Definitions of the symbols are included in the descriptions of the characteristics.

1. The intensity is only as much as the machines can deliver. That is, there is no such thing as negative intensity:

$$x \geq 0 \quad (\text{Eq 3})$$

and there is a maximum intensity,  $g$ :

$$x \leq g \quad (\text{Eq 4})$$

These two inequalities can be written together as:

$$0 \leq x \leq g \quad (\text{Eq 5})$$

2. The rate of change of intensity is within the machine limits,  $w$ .  $Sx$  is an estimate of the derivative of the intensity:

$$-w \leq Sx \leq w \quad (\text{Eq 6})$$

3. The resulting shape is exactly right if

$$Dx = t \quad (\text{Eq 7})$$

where  $D$  is the displacement matrix of stress influences generated by the finite element analysis module, and  $t$  is the target shape.

4. The resulting shape is within a specified tolerance,  $\epsilon$ , of the right shape:

$$-\epsilon \leq Dx - t \leq \epsilon \quad (\text{Eq 8})$$

or equivalently:

$$t - \epsilon \leq Dx \leq t + \epsilon \quad (\text{Eq 9})$$

Note that in the descriptions of the characteristics,  $x, g, w, t$ , and  $\epsilon$  are vectors and  $D$  and  $S$  are matrices.

Typically  $D$  has more columns than rows, so we would expect to have infinitely many solutions to characteristic 3. Experience has shown, however, that frequently there is no solution to “get the right shape” as an equality. And even if there is a solution to characteristic 3, it may not satisfy characteristics 1 and 2. Therefore, we use characteristic 4 instead of 3 during the design process.

### 3.2 Finding an Optimal Pattern

We developed a set of questions and problem formulations that could be used to understand a particular peening problem. Mathematically we have to decide how to fill in the templates described in Eq 1 and 2. The choice is which characteristics to put into the objective function and which characteristics to use as constraints in the LCLS template. Note that for a particular problem there can be only one objective function, but there can be many constraints. The solution to the FP problem, if it exists, may be one of many. Using the LCLS formulations we try to pick out the particular solution of interest. However, even with the LCLS formulations there may be many solutions.

First, we look for acceptable patterns, where an *acceptable* pattern is one that is producible (characteristics 1 and 2) and results in a shape that is within a specified tolerance (characteristic 4). Pick  $\epsilon$  to be the maximum allowable variation between the peened shape and the target shape. We find acceptable patterns by solving:

$$\text{FP: Find } x \text{ to satisfy } \begin{cases} 0 \leq x \leq g \\ -w \leq Sx \leq w \\ (t - \epsilon) \leq Dx \leq (t + \epsilon) \end{cases} \quad (\text{Eq 10})$$

If there is a solution to this problem, then we are assured that it uses only as much intensity as the machine can deliver and that it does not change the intensity any faster than the machine can. At this point there may be many feasible solutions. We can use the LCLS problem formulations to find the “best” point. If Eq 10 has no solution, then we cannot use peening to get the shape we want. We can use the other problem formulations described later in this section to help understand why.

In the case when there are many acceptable solutions, we do not have a single definition of “best,” but we can look at three clear alternatives. Each one uses a different characteristic as the objective function but keeps the same acceptability constraints. It would be useful to solve all three to see the difference in the patterns and to get the values for the objective functions.

What acceptable pattern gets closest to the target shape? To answer this question we solve the following:

$$\text{LCLS: Find } x \text{ to minimize } \frac{1}{2} \|Dx - t\|^2 \\ \text{subject to } \begin{cases} 0 \leq x \leq g \\ -w \leq Sx \leq w \\ (t - \epsilon) \leq Dx \leq (t + \epsilon) \end{cases} \quad (\text{Eq 11})$$

Comparing Eq 11 to template 1, we have chosen a measure of the difference between the peened shape and the target shape as the object function. The constraints are the acceptability constraints from Eq 10.

What acceptable pattern is the smoothest? To answer this question we solve the following:

LCLS:

$$\text{Find } x \text{ to minimize } \frac{1}{2} \|Sx\|^2 \\ \text{subject to } \begin{cases} 0 \leq x \leq g \\ -w \leq Sx \leq w \\ (t - \epsilon) \leq Dx \leq (t + \epsilon) \end{cases} \quad (\text{Eq 12})$$

The only difference between Eq 11 and 12 is that we have chosen a different objective function. In Eq 12 the objective function is a measure of the smoothness of the pattern.

What acceptable pattern uses the smallest average intensity? To answer this question we solve the following:

LCLS:

$$\text{Find } x \text{ to minimize } \frac{1}{2} \|Ix\|^2 \\ \text{subject to } \begin{cases} 0 \leq x \leq g \\ -w \leq Sx \leq w \\ (t - \epsilon) \leq Dx \leq (t + \epsilon) \end{cases} \quad (\text{Eq 13})$$

where  $I$  is the identity matrix.

Again, the only difference between Eq 13, 12, and 11 is the objective function. In Eq 13 the objective function is a measure of the total intensity used to provide the pattern.

Finally we can minimize intensity and get close to the target shape in one problem, as follows:

LCLS:

$$\text{Find } x \text{ to minimize } c^T x + \frac{1}{2} \|Dx - t\|^2 \\ \text{subject to } \begin{cases} 0 \leq x \leq g \\ -w \leq Sx \leq w \\ (t - \epsilon) \leq Dx \leq (t + \epsilon) \end{cases} \quad (\text{Eq 14})$$

This is difficult to do because we do not know how to select the weighting vector  $c$ . Perhaps a better choice is to solve Eq 11 to 13, look at the results, and use the values of the objective functions to choose new values for  $g$ ,  $c$ , and  $w$ . For example, solve Eq 13 and use the value of the objective function to get a new value for  $g$ . Use the new value to solve Eq 11 and 12. This way we can explicitly control the trade-off between intensity, smoothness, and deviation from target shape.

If Eq 10 has no solution then we could increase the values for  $g$ ,  $w$ , and  $c$  and cycle through solving Eq 11 to 13.

## 4. Conclusions

A numerical model has been developed to replicate the shot peening process as it applies to the forming of aircraft wing skins. The model uses the finite element method coupled with empirical relationships for induced stress due to the peening process. To arrive at an optimal solution, several criteria must be simultaneously satisfied. These criteria include peening intensity limits, form fit criteria, and smoothness limits. Several LSSOL formulations are presented for attempting the optimal solution. Tests have been performed using cylindrical wings as well as actual production wing shapes, and the numerical model yields encouraging results.

## Acknowledgments

The first author gratefully acknowledges the Boeing Commercial Airplane Group for the knowledge, time, material, and support which they so graciously gave.

## References

1. "Shot Peening of Metal Parts," MIL-S-13165C, U.S. Army Command Laboratory
2. Shot Peening, *Metals Handbook*, 9th ed., Vol 5, American Society for Metals, 1982, p 138-149
3. *Mechanical Engineer's Handbook*, John Wiley & Sons, 1986, p 942-951
4. D.V. Nelson, R.E. Ricklefs, and W.P. Evans, The Role of Residual Stresses in Increasing Long-Life Fatigue Strength of Notched Machine Members, *Achievement of High Fatigue Resistance in Metals and Alloys*, STP 467, American Society for Testing and Materials, 1970, p 228-253
5. P.G. Feld and D.E. Johnson, Advanced Concepts of the Process, "Shot Peening for Advanced Aerospace Design," SP-528, Society of Automotive Engineers, 1982, p 19-22
6. S.E. Homer and R.D. VanLuchene, Aircraft Wing Skin Contouring by Shot Peening, *J. Mater. Shaping Technol.*, Vol 9, 1991, p 1-13
7. S.T.S. Al-Hassani, Mechanical Aspects of Residual Stress Development in Shot Peening, *Proc. First International Conference on Shot Peening*, Pergamon Press, Sept 1981, p 583-602
8. S.T.S. Al-Hassani, The Shot Peening of Metals—Mechanics and Structures, "Shot Peening for Advanced Aerospace Design," SP-528, Society of Automotive Engineers, 1982, p 23-28
9. O.C. Zienkiewicz and R.L. Taylor, *The Finite Element Method*, 4th ed., McGraw-Hill, 1991, p 114-120
10. P.G. Bergan and C.A. Felippa, A Triangular Membrane Element with Rotational Degrees of Freedom, *Computer Methods in Applied Mechanics and Engineering*, Vol 50, 1985, p 25-69
11. C.C. Rankin and F.A. Brogan, An Element Independent Corotational Procedure for the Treatment of Large Rotations, *J. Pressure Vessel Technol.*, Vol 108, May 1986, p 165-174
12. J. Argyris, An Excursion into Large Rotations, *Computer Methods Appl. Mech. Eng.*, Vol 32, 1982, p 85-155
13. P.E. Gill, S.J. Hammarling, W. Murray, M.A. Saunders, and M.H. Wright, "Users Guide for LSSOL (Version 1.0): A FORTRAN Package for Constrained Linear Least-Squares and Convex Quadratic Programming," Technical Report SOL 86-1, Department of Operations Research, Stanford University, 1986
14. J.J. More and S.J. Wright, *Optimization Software Guide*, Society for Industrial and Applied Mathematics, 1993
15. E.J. Cramer, "Optimization and Data Modelling for Shot Peening," Technical Report BCSTECH-93-046, Boeing Computer Services, 1993